



Published in final edited form as:

Neurorehabil Neural Repair. 2014 June ; 28(5): 433–442. doi:10.1177/1545968313516868.

Handgrip-related activation in primary motor cortex relates to underlying neuronal metabolism after stroke

Carmen M. Cirstea, MD, PhD^{a,c,d,1,*}, Cary R. Savage, PhD^e, Randolph J. Nudo, PhD^{b,f}, Leonardo G. Cohen, MD^h, Hung-Wen Yeh, PhD^g, In-Young Choi, PhD^{a,d,f}, Phil Lee, PhD^{a,f}, Sorin C. Craciunas, MD, PhD^{a,2}, Elena A. Popescu, PhD^a, Ali Bani-Ahmed, PhD^{a,c}, and William M. Brooks, PhD^{a,d}

^aHoglund Brain Imaging Center, University of Kansas Medical Center

^bLandon Center on Aging, University of Kansas Medical Center

^cDepartment of Physical Therapy and Rehabilitation Science, University of Kansas Medical Center

^dDepartment of Neurology, University of Kansas Medical Center

^eDepartment of Psychiatry and Behavioral Sciences, University of Kansas Medical Center

^fDepartment of Molecular and Integrative Physiology, University of Kansas Medical Center

^gDepartment of Biostatistics, University of Kansas Medical Center

^hDepartment of Human Cortical Physiology Section and Stroke Neurorehabilitation Clinic, National Institute of Neurological Disorders and Stroke NIH

Abstract

Background—Abnormal task-related activation in primary motor cortices (M1) has been consistently found in functional imaging studies of subcortical stroke. Whether the abnormal activations are associated with neuronal alterations in the same or homologous area is not known.

Objective—Our goal was to establish the relationships between M1 measures of motor task-related activation and a neuronal marker, N-acetylaspartate, in patients with severe to mild hemiparesis.

Methods—Eighteen survivors of an ischemic subcortical stroke (confirmed on T2-weighted images) at more than six months post-onset and sixteen age- and sex-matched right-handed healthy controls underwent functional MRI during a handgrip task (impaired hand in patients, dominant hand in controls) and proton magnetic resonance spectroscopy (¹H-MRS) imaging. Spatial extent and magnitude of blood oxygen level-dependent response (or activation) and N-

*Corresponding author: Carmen M. Cirstea, MD, PhD Departments of Psychological Sciences and Physical Medicine & Rehabilitation University of Missouri Brain Imaging Center, 205d Melvin H. Marx Building 1416 Carrie Francke Drive Columbia, MO 65211 Office: 573-884-4737 Fax: 573-884-3560 cirsteac@missouri.edu.

¹Current address: Departments of Psychological Sciences and Physical Medicine & Rehabilitation, Brain Imaging Center & Rehabilitation Neuroscience Lab, University of Missouri

²Current address: Neurosurgery Unit IV, Bagdasar-Arseni Hospital

Disclosure/Conflict of Interest

No duality of interest to declare.

acetylaspartate levels were measured in each M1. Relationships between activation and N-acetylaspartate were determined.

Results—Compared to controls, patients had greater extent of contralesional (ipsilateral to impaired hand, $p < .001$) activation, higher magnitude of activation and lower N-acetylaspartate in both ipsilesional ($p = .008$ and $p < .001$ respectively) and contralesional ($p < .0001$, $p < .05$) M1. There were significant negative correlations between extent of activation and N-acetylaspartate in each M1 ($p = .02$) and a trend between contralesional activation and ipsilesional N-acetylaspartate ($p = .08$) in patients but not in controls.

Conclusions—Our results suggest that greater neuronal recruitment could be a compensatory response to lower neuronal metabolism. Dual-modality imaging may be a powerful tool for investigating relationships between complementary data regarding post-stroke brain reorganization.

Keywords

subcortical stroke; primary motor cortex; $^1\text{H-MRS}$; fMRI; functional-biochemistry relationship

Introduction

Stroke remains the leading cause of motor disability among adults. A major contributor to disability is persistent arm/hand motor impairment. Stroke survivors show altered brain activation patterns in both hemispheres on functional imaging studies. Specifically, execution of simple movements with the impaired arm is associated with increased activation in ipsilesional (same as the stroke) non-motor areas, contralesional (opposite to the stroke) motor areas, and bilateral premotor areas. Successful recovery occurs in patients who return to relatively normal patterns of brain activation, whereas patients who show persistent bilateral cortical activation typically have poorer recovery.

Although the normalization of activation in the ipsilesional M1 (iM1) is generally associated with return of arm motor function, the relationship between contralesional M1 (cM1) activation and arm motor recovery remains under debate. Studies using transcranial magnetic stimulation or cathodal transcranial direct current stimulation suggest that cM1 is recruited to compensate for damaged crossed pathways. Some argue that the cM1 recruitment reflects the recruitment of un-crossed pathways, although there is no evidence that contralesional activation represents firing of uncrossed corticospinal tract (CST) fibers, which would be expected to involve proximal rather than distal movements. Contralesional M1 recruitment might also represent an epiphenomenon reflecting either a diffuse recruitment of the motor networks driven by higher orders areas during a task performance, or a dendritic overgrowth due to overuse of the healthy hand. Hence, although the exact role of cM1 in recovery remains elusive, interactions between cM1 and iM1 are likely to be critical for motor recovery, particularly in patients with poor recovery.

Although the neural mechanisms underlying the M1 functional changes after stroke remain largely unknown, non-invasive proton magnetic resonance spectroscopy ($^1\text{H-MRS}$) studies have found lower M1 levels of N-acetylaspartate (NAA), particularly in the ipsilesional

hemisphere⁻. Though the precise biological function remains uncertain, reduced NAA levels are thought to index neuronal loss, dysfunction, or both. This suggests that changes in activation of the M1 may be a consequence of, or a compensation for, an underlying neuronal impairment. However, no study to date has acquired these measures within the same area in the same patient.

In the present study, we sought to clarify the neural basis underlying the activation changes seen in chronic subcortical stroke using a combined fMRI and ¹H-MRS approach. We focused primarily on the primary motor cortex (M1), given previous evidence of its major involvement in motor recovery after stroke⁻. For the fMRI paradigm, we used the handgrip task that has been shown to robustly activate M1⁻. We then acquired ¹H-MRS measures from the activated M1 regions. Based on previous work, we hypothesized that patients would show increased handgrip-related activation, particularly in cM1, and decreased NAA levels in both M1s. We also determined the relationships between activation and NAA within and between M1s. We hypothesized that inverse relationships would constitute evidence in support of compensatory M1 activation driven by a neuronal impairment.

Methods

Participants

Eighteen right-handed stroke patients and 16 right-handed healthy controls provided written informed consent to this study, which was approved by the institutional ethics committee. Of these, 11 patients and 10 controls participated in an earlier study that explored M1 neurochemical levels.

Patients were required to have a first-ever ischemic subcortical stroke at least six months previously, have M1 intact on T2-weighted magnetic resonance imaging (MRI), and be able to perform a handgrip task (Fugl-Meyer Upper Extremity Scale (FMUE) \geq 10). Patients were also required to understand simple instructions (Token test) and have no visual attention deficits (Cancellation test), apraxia (clinical observation of the use of scissors to cut paper and making coffee), or other neurological or psychiatric diseases. Patients were on anti-hypertensive (75%), cholesterol-lowering (62%), and/or antiplatelet (81%) therapy, but were not receiving rehabilitation treatment.

Age-, sex-, and education-matched healthy controls, without neurological or psychiatric disorders, participated.

Patients attended an initial screening session to assess arm motor impairment using FMUE (where a score of 66 indicates no impairment). All participants completed one magnetic resonance imaging (MRI) session, including brain structural, functional, and ¹H-MRS imaging (3T Allegra MR system, Siemens Medical Solutions, Erlangen, Germany). The total duration for the MRI session was about 45 min. Full details of the MRI protocol appear elsewhere⁻.

Structural MRI

Two structural data sets were acquired, T1-weighted structural (TR=2300ms; TE=3ms; FOV=240mm; matrix=256×256; resolution=1×1×1mm³) and T2-weighted structural (TR=4800ms; TE1/TE2=18/106ms; FOV=240mm; matrix=256×256; slice thickness=5mm, no gap), to: (i) confirm lesion location, (ii) exclude other pathological conditions, (iii) estimate the brain tissue volume in spectroscopic voxels (see below), (iv) quantify lesion volume: Lesions were defined as tissue having abnormal high signal on T₂-weighted images and as subcortical if they include >50% of subcortical tissue. We manually traced the lesion slice-by-slice on axial T2-weighted images (MedINRIA, Cedex, France, www.sop.inria.fr/asclepios/software/MedINRIA/). Finally, we estimated the volume using MIPAV (<http://mipav.cit.nih.gov/>); (v) identify white matter hyperintensities (WMH; the Fazekas scale: range 0 to 3, 0 and 1 being considered normal in the elderly); and (vi) estimate global grey matter volume (SIENAX).

Functional MRI

Blood Oxygenation Level Dependent (BOLD; TR=2000ms; TE=50ms; 25 slices; slice thickness=5mm; 0 skip; 100 data points; resolution: 5×5mm²) was acquired while performing a visually-cued handgrip, as described previously. For this task, we used an MRI-compatible device, consisting of an air-filled polymer bulb connected to a pressure transducer (placed outside of the scanner field). During the handgrip, pressure values were detected by transducer and presented graphically to the participant (LabVIEW 7.1, National Instruments, Texas). Patients performed the task with the impaired hand and controls used the right (dominant) hand. Since the ability to perform handgrip returns earlier than fractionated finger movements, handgrip task is a well-suited task to study patients with a wide range of recovery. Thus, we were able to study patients with mild to severe hemiparesis.

Each participant's maximal voluntary contraction (MVC) on the handgrip task was measured prior to scanning. Participants generated MVC on three five-second trials; the highest peak pressure produced was used as the MVC. During scanning, a target pressure of 25% of MVC was displayed graphically while participants performed the handgrip task. This target pressure was used to control for effort across all participants. Upon reaching the target pressure, the grip was released. Practice outside the scanner minimized unwanted movements and made the participant comfortable with the task.

We used a block design consisting of two alternating conditions, movement and rest. In the movement condition, each handgrip was cued by the appearance of the word 'MOVE'. In the resting condition, participants were instructed (by word cue 'STOP') to remain motionless. The word cue was repeated five times, every 4s, for each condition (20s each) and the run consisted of 25 cued events (handgrip) and 25 null events (one run=3min 28s).

BOLD data analysis

The fMRI analysis was performed off-line using Brain Voyager software (Brain Innovation B.V., Maastricht, Netherlands). The first 2 volumes of each scan were discarded to avoid T₁ saturation effects. Preprocessing included motion correction using rigid body

transformation, estimating six parameters (three translational and three rotational). Inspection of these parameters found that none of the participants moved their head more than 2 mm in any direction; spatial smoothing using 4mm Gaussian filter, to permit valid statistical inferences based on Gaussian random field theory; mean-based intensity normalization of all volumes by the same factor; and high-pass temporal filtering at 0.01Hz, to remove low frequency confounds.

Without knowledge of the activation patterns, M1 was outlined on the coincident T₁-weighted image using standard sulcal and gyral landmarks: anterior bank of the central sulcus with the caudal border lying in the depth of the central sulcus close to its fundus and anterior border abutting Brodmann area 6, and the total voxels was counted for each M1. We then counted the activated voxels in M1 using a Bonferroni corrected p=0.01 (see below). The ratio between the number of activated voxels and the total voxels in each M1 represents the spatial extent of activation (SEA). The general linear model was used to contrast BOLD signal between movement and rest conditions, modeled by a boxcar function with hemodynamic response modification (predictor movement). The voxel values were considered significant if the activation survived a Bonferroni-corrected significance threshold of 0.01. We selected a cluster of 100 contiguous voxels for hand representation in each M1. Signal intensity versus time curves were examined for each significant activation and a mean signal change (or MSC) in movement vs. rest condition was calculated.

Proton magnetic resonance spectroscopy imaging (¹H-MRSI)

Immediately after the BOLD acquisition was completed, we analyzed the fMRI results using the scanner analysis software to locate the M1 activation for ¹H-MRSI positioning. These results were not used for the subsequent analyses. Point Resolved Spectroscopy or PRESS was used (TE=30ms; TR=1500ms; FOV=160mm²; matrix=16×16; slice thickness=15mm; in-plane resolution=5×5mm²; spectral width=1200Hz). We minimized lipid artifact from the scalp by using eight outer voxel suppression bands (thickness=30 mm) around the volume of interest. We used automatic and manual shimming to achieve full-width at half maximum of <20Hz of the water signal from the entire excitation volume.

NAA concentrations were calculated using LCModel. Using custom-designed software (Matlab v7.1) to overlay the LCModel output, BOLD images, and segmented T₁-weighted images (SPM2 Department of Cognitive Neurology, London, UK), we selected three spectroscopic voxels in the hand representation in M1 with a signal-to-noise ratio >10 and >75% brain tissue (BT, grey+white matter from SPM2 segmentation) and NAA Cramer-Rao lower bounds <20%. If M1 activation was absent, we selected the spectroscopic voxels corresponding to the “hand knob” in M1 (<http://neuro.imm.dtu.dk/services/jerne/ninf/voi.html>) (Fig. 1A).

We corrected metabolite concentrations as follows: $c = c_{\text{LCModel}} / \text{BT}$ where c is the BT-corrected concentration, c_{LCModel} is the concentration in institutional units (from LCModel), and BT is the estimated brain tissue. The BT-corrected concentration was then converted into molar concentrations (millimoles per kilogram wet weight brain tissue).

Statistical analysis

Variables (demographic: age, years of education; clinical: FMUE scores, time post-stroke, lesion volume, WMH, global grey matter volume) and M1 outcomes (primary: NAA, SEA; secondary: MSC) were described by means and standard deviations. Since lesion volume was not normally distributed, we used a logarithmic transform. To quantify differences in SEA and MSC between M1s, we used the activation laterality index (LI = (C-I)/(C+I), where C and I represents the contralateral M1 SEA (MSC) or ipsilateral M1 SEA (MSC) to the hand performing the motor task, respectively. The LI can range from 1.0 (all activity in the contralateral M1) to -1.0 (all activity in the ipsilateral M1).

Between-group differences in demographic variables and M1 outcomes were explored using parametric (t-test) or non-parametric (Wilcoxon rank-sum test) statistics, depending on their distributions.

Within group, between-hemisphere differences in variables were assessed using 2-tailed paired t-tests. We used Spearman rank order correlation to analyze the relationships between (i) primary outcomes and clinical variables, and (ii) SEA, MSC, and NAA within and across M1. The significance level was set at $p < 0.05$ (SPSS 18.0, SPSS Inc. Chicago, IL).

Results

Participant characteristics

Patients—Stroke survivors had experienced a single subcortical infarction between 6 and 144 months prior to scanning (mean \pm SD=37.4 \pm 36.7mo) leading to moderate arm paresis (FMUE=42.9 \pm 16.9). Lesion volume varied from 180mm³ to 25,340mm³ (8,575.4 \pm 15,239.0mm³). Twelve patients had left-sided infarcts. Fourteen survivors had infarcts in the basal ganglia, with extension to posterior limb of the internal capsule (PLIC) in seven patients, to anterior limb (ALIC) in three patients, to both PLIC and ALIC in two patients, and to corona radiata in five patients. One patient had an infarct in the PLIC with extension to thalamus, one had an ALIC infarction, one survivor had cerebral peduncles infarction, and one had an infarct in pons. Fazekas scores varied between 0 and 1 (Table 1).

Patients vs. Controls—Age (57.4 \pm 9.1 vs. 49.9 \pm 13.7yrs, *NS*), male/female distribution (12/6 vs. 10/6, *NS*), or years of education (13.6 \pm 1.7 vs. 14.0 \pm 2.5yrs, *NS*) did not differ between patients and controls. We compared the iM1 to the left M1 (IM1) from controls based on (i) lack of M1 NAA lateralization in healthy, (ii) similar handgrip activations for both dominant and non-dominant hands in healthy, and (iii) most (67%) of our patients had left hemisphere injury.

Spatial extent of handgrip-related activation in primary motor cortex

Controls—A robust contralateral BOLD response was seen in all controls while using the right (dominant) hand (IM1, 13.0 \pm 8.8% of total IM1, Fig. 1B for range of SEA). Ipsilateral, i.e., right, M1 activation was significantly smaller (0.6 \pm 1.4%, $p < .001$) and was recorded in only 5 out of 16 controls. The LI was 0.9, suggesting dominant contralateral M1 activation.

Patients—Patients consistently activated both M1s while using the impaired arm (iM1, $18.6\pm 14.7\%$; cM1, $13.0\pm 11.2.0\%$). No significant differences between iM1 activation and cM1 activation were found ($p=.2$).

Spatial extent of M1 activation was significantly correlated with FMUE scores, but not with lesion volume, global grey matter volume, or time after stroke (Table 2).

Subgroup analysis (Table 3) showed no significant differences in M1 activation based on stroke lateralization, left vs. right hemisphere, or internal capsule location, PLIC vs. ALIC.

Patients vs. controls—Although patients, as a group, generally activated a larger iM1 than controls, this did not reach statistical significance ($p=.2$). Five out of 18 patients showed greater SEA than the range recorded from uninjured group (Fig. 1B). As expected, cM1 SEA in patients was considerably greater than in controls ($13.0\pm 11.2\%$ vs. $0.6\pm 1.4\%$, $p<.001$). Eleven patients activated more cM1 compared to the range of our control group (Fig. 1B). We also found altered lateralization for the patient group. The LI was 0.2, reflecting an increased involvement of cM1.

Magnitude of handgrip-related activation in primary motor cortex

Patients vs. controls—The magnitude of M1 activation, as measured by MSC, was significantly higher in patients than in controls (iM1: $0.9\pm 0.3\%$ vs. lM1, $0.7\pm 0.2\%$, $p=.008$; cM1: $0.8\pm 0.7\%$ vs. rM1, $0.01\pm 0.02\%$, $p<.001$). Activation was also less lateralized in patients compared to controls (LI: 0.05 vs. 0.95 in controls), similar to the results for SEA (see above).

N-acetylaspartate levels in primary motor cortex

$^1\text{H-MRS}$ spectra with good signal-to-noise ratios were obtained consistently from both control and stroke participants. Similar percentages of brain tissue within spectroscopic voxels were found between groups (iM1: $89.0\pm 6.2\%$ vs. lM1, $88.8\pm 7.2\%$, $p=.9$; cM1: $87.0\pm 7.9\%$ vs. rM1, $88.9\pm 5.0\%$, $p=.4$).

Controls—Consistent with our previous findings, similar NAA levels were found in lM1 and rM1 in healthy controls ($11.5\pm 1.4\text{mM}$ vs. $11.7\pm 1.9\text{mM}$, $p=.8$; see Fig. 1C for range of NAA).

Patients—Ipsilesional NAA was significantly lower than contralesional NAA ($9.5\pm 1.4\text{mM}$ vs. $10.4\pm 1.6\text{mM}$, $p=.02$). Significant positive correlations were found between NAA and FMUE (Table 2), suggesting that NAA is lower in both M1s in patients with poorer outcomes (Fig. 1C). There were no significant correlations between NAA and stroke volume, global grey matter volume, or time post-stroke (Table 2). NAA levels were not significantly different in left vs. right stroke or in PLIC vs. ALIC stroke (Table 3).

Patients vs. controls—Mean NAA levels in each M1 in patients were significantly lower than those in controls (iM1 vs. lM1 $p<.001$; cM1 vs. rM1 $p<.05$).

Relationships between spatial extent and magnitude of activation and NAA levels in primary motor cortex

Controls—No significant correlations were detected between SEA and NAA level within lM1 (Spearman $r=-0.17$, $p=.5$) or rM1 ($r=0.36$, $p=.2$) nor between MSC and NAA (lM1, $r=-0.08$, $p=.8$; rM1, $r=-0.04$, $p=.9$).

Patients—In contrast, patients showed a significant negative correlation between SEA and NAA in each M1 (ipsilesional, $r=-0.55$, $p=.02$; contralesional, $r=-0.53$, $p=.02$; Fig. 2, upper row). Patients showed weaker negative correlation between cM1 SEA and iM1 NAA levels ($r=-0.42$, $p=.08$, Fig. 2A, lower row). Although correlations between MSC and NAA within or across M1s were all negative, similar to SEA, (iM1, $r=-0.14$, $p=.6$; cM1, $r=-0.38$, $p=.1$; iM1 MSC -cM1 NAA, $r=-0.24$, $p=.4$; cM1 MSC -iM1 NAA, $r=-0.42$, $p=.1$), they did not reach statistical significance.

Discussion

Although numerous studies have used either fMRI or $^1\text{H-MRS}$ to examine brain reorganization after stroke, to our knowledge this is the first report that integrates these modalities to investigate the relationships between activation and neuronal metabolism measures in M1 after stroke.

Handgrip-related activation in primary motor cortex in chronic subcortical stroke

As reported in previous studies⁷, the activation pattern associated with impaired hand movement consistently included both ipsilesional and contralesional M1. Our data also showed that a greater motor deficit is associated with a greater bilateral M1 activation⁷. Increased ipsilesional activation is likely to reflect a recruitment of larger pool of neurons with intact axons probably due to a loss of recurrent inhibition onto surrounding pyramidal cells, changes in the properties of existing neuronal pathways, and/or changes in anatomical connections between areas. Our finding of greater contralesional activation might be due to altered inter-hemispheric inhibition, dendritic overgrowth due to overuse of the healthy hand, recruitment of un-crossed CST fibers recruitment⁷, and/or mirror movements. An alternative explanation might be that patients with poor motor outcome might perceive the task as more complex resulting in greater bilateral M1 activation. Although the effort levels of our task were matched at 25% of individual MVC, we did not control attention. Thus, we cannot rule out the possibility that attention differences contributed to larger M1 activations.

N-acetylaspartate in primary motor cortex in chronic subcortical stroke

Our second finding of lower NAA corroborates prior reports in stroke⁷. Although the specific mechanism underlying lower NAA remains the topic of some conjecture, dysfunctional neurons may contain lower NAA due to less synthesis and/or release. Indeed, in ipsilesional M1, dysfunctional neurons could result from distal ischemic axotomy⁷ and/or diaschisis, i.e., depressed neural activity in brain regions distant but structurally or functionally connected to the damaged brain area⁷. Although it is unknown whether biochemical and/or electrophysiological changes described in surviving neurons with ischemic axotomy⁷ are similar to those classically described in diaschitic neurons, these

changes are likely to be associated with impaired mitochondrial function, and hence NAA decline. The concept of metabolically depressed neurons is further supported by observation of morphological and biochemical cell body changes after axonal injury, indicating that neurons shift from “transmitting” to “degenerative/regenerative” state. Our findings of lower NAA in the contralesional M1, also confirm our prior work and might result from trans-hemispheric diaschisis.

Other explanations for lower NAA are also possible. NAA is involved in myelin/fatty acid synthesis and osmotic regulation, but these processes are unlikely to be altered in normal appearing cortex remote from the injury. Lower NAA can also result from dead neurons. However, neuronal loss seems unlikely in M1 since there is little evidence of retrograde degeneration or cortical cell death after subcortical stroke. Moreover, we found no differences in brain tissue volume in the spectroscopic voxels in patients compared to controls, which would be expected in the context of appreciable neuronal loss. Therefore, although lower NAA levels potentially reflect a variety of underlying mechanisms, in the context of the present findings, we consider that lower NAA levels suggest metabolically depressed neurons.

Correlation between handgrip-related activation and N-acetylaspartate in primary motor cortex in chronic subcortical stroke

Our third finding of a negative correlation between extent of activation and NAA levels in each M1 suggests that the amount of neuronal recruitment during a motor task is related to the magnitude of M1 metabolic abnormality. We speculate that the morphological and biochemical cell body changes after axonal injury in the ipsilesional M1, noted above, associated with increased synthesis of proteins associated with growth may support formation of new local intracortical connections. For instance, these could recruit adjacent neurons with intact axons, i.e., pyramidal tract neurons, which potentially have similar muscle projections as the metabolically depressed neurons. Similarly, the changes in neuronal morphology in the contralesional M1 could be associated with a larger neuronal recruitment in this area. Moreover, the contralesional recruitment was also negatively correlated to ipsilesional NAA, suggesting that as the ipsilesional M1 neuronal compartment is increasingly compromised, the more contralesional M1 is recruited. This result is supported by recent findings that contralesional M1 activation correlates with ipsilesional motor pathway integrity. This is a novel finding that requires further attention.

An alternative strategy for investigating BOLD activations is to examine the magnitude of signal changes. Our results are generally consistent with those from the SEA analysis discussed above i.e., the NAA levels were also negatively correlated to a modest extent with the magnitude of activation. Further studies are needed to elucidate the relationships between the BOLD signal and the physiological role of NAA in neurons.

Nevertheless, these findings help us to rule out the contribution of attention or mirror movements to enlarged M1 activation, as we would not expect underlying neuronal disturbances in the areas regularly recruited during normal motor programming. Further, contralesional dendritic overgrowth could be also omitted from our interpretation, based on our findings of lower contralesional M1 NAA levels.

Study limitations

We recruited a relatively large sample for a study of this type, i.e., imaging study after stroke. Since this was the first study to use a dual-imaging modality approach, we increased our statistical power by recruiting only survivors of sub-cortical stroke and examining only one cortical motor area, M1. We also chose to examine only one neurometabolite, NAA and asked a series of very focused questions. Nonetheless, there were some limitations. The focus on subcortical infarcts provides statistical power by minimizing patient variance, but limits our ability to explore the effects of infarct location on the relationships brain function-biochemistry. Similarly, since our analysis focused on M1, we cannot comment on the involvement of other brain regions that are critical to stroke recovery. Our focus on NAA means that we can make no comment on other brain metabolites such as glutamate and GABA. Clearly, future studies of the relationship between these metabolites and motor performance and recovery would be of great interest.

Our data could be explained, in part, by resting cerebral blood flow alterations, perhaps resulting from carotid stenosis. However, there is evidence that reduced resting cerebral blood flow also results in elevated choline and lactate, which were not significantly altered in our sample (results not shown). Thus, we consider that carotid stenosis is not a significant contributor to our findings.

Finally, due to the point-spread function of $^1\text{H-MRSI}$, the effective voxel size is bigger than the nominal voxel size. Thus, we cannot rule out the possibility that our measurements include more than hand representation in each area.

Summary

Although overlapping processes underly functional M1 changes after stroke, our findings suggest that one factor could be the altered neuronal metabolism in these areas. Thus, we advocate that functional MRI and $^1\text{H-MRS}$ provide complementary probes of cerebral tissue that, when used together, improve our understanding of the cellular substrate of brain reorganization after stroke. Further use of such combined approaches might help us to better understand the mechanisms of recovery and develop better therapeutic approaches.

Acknowledgments

Sources of Funding: This work was supported by American Heart Association (0860041Z to CMC; 0655759Z to WMB). The Hoglund Brain Imaging Center is supported by a generous gift from Forrest and Sally Hoglund and National Institutes of Health (P30 AG 035382, P30 HD 002528, and UL1 TR000001). The contents are solely the responsibility of the authors and do not necessarily represent the official views of the NIH or its institutes.

References

1. Feigin VL, Lawes CM, Bennett DA, Barker-Collo SL, Parag V. Worldwide stroke incidence and early case fatality reported in 56 population-based studies: a systematic review. *Lancet Neurol.* 2009; 8:355–369. [PubMed: 19233729]
2. Lai SM, Studenski S, Duncan PW, Perera S. Persisting consequences of stroke measured by the Stroke Impact Scale. *Stroke.* 2002; 33:1840–1844. [PubMed: 12105363]

3. Weiller C, Ramsay SC, Wise RJ, Friston KJ, Frackowiak RS. Individual patterns of functional reorganization in the human cerebral cortex after capsular infarction. *Ann Neurol.* 1993; 33:181–189. [PubMed: 8434880]
4. Nelles G, Contois KA, Valente SL, et al. Recovery following lateral medullary infarction. *Neurology.* 1998; 50:1418–1422. [PubMed: 9595998]
5. Ward NS, Brown MM, Thompson AJ, Frackowiak RS. Neural correlates of outcome after stroke: a cross-sectional fMRI study. *Brain.* 2003; 126:1430–1448. [PubMed: 12764063]
6. Cramer SC, Nelles G, Benson RR, et al. A functional MRI study of subjects recovered from hemiparetic stroke. *Stroke.* 1997; 28:2518–2527. [PubMed: 9412643]
7. Johansen-Berg H, Rushworth MF, Bogdanovic MD, Kischka U, Wimalaratna S, Matthews PM. The role of ipsilateral premotor cortex in hand movement after stroke. *Proc Natl Acad Sci U S A.* 2002; 99:14518–14523. [PubMed: 12376621]
8. Marshall RS, Perera GM, Lazar RM, Krakauer JW, Constantine RC, DeLaPaz RL. Evolution of cortical activation during recovery from corticospinal tract infarction. *Stroke.* 2000; 31:656–661. [PubMed: 10700500]
9. Ward NS, Brown MM, Thompson AJ, Frackowiak RS. Neural correlates of motor recovery after stroke: a longitudinal fMRI study. *Brain : a journal of neurology.* 2003; 126:2476–2496. [PubMed: 12937084]
10. Johansen-Berg H, Dawes H, Guy C, Smith SM, Wade DT, Matthews PM. Correlation between motor improvements and altered fMRI activity after rehabilitative therapy. *Brain.* 2002; 125:2731–2742. [PubMed: 12429600]
11. Calautti C, Naccarato M, Jones PS, et al. The relationship between motor deficit and hemisphere activation balance after stroke: A 3T fMRI study. *Neuroimage.* 2007; 34:322–331. [PubMed: 17045490]
12. Takeuchi N, Tada T, Toshima M, Chuma T, Matsuo Y, Ikoma K. Inhibition of the unaffected motor cortex by 1 Hz repetitive transcranial magnetic stimulation enhances motor performance and training effect of the paretic hand in patients with chronic stroke. *J Rehabil Med.* 2008; 40:298–303. [PubMed: 18382826]
13. Fregni F, Pascual-Leone A. Hand motor recovery after stroke: tuning the orchestra to improve hand motor function. *Cogn Behav Neurol.* 2006; 19:21–33. [PubMed: 16633016]
14. Nowak DA, Grefkes C, Dafotakis M, et al. Effects of low-frequency repetitive transcranial magnetic stimulation of the contralesional primary motor cortex on movement kinematics and neural activity in subcortical stroke. *Arch Neurol.* 2008; 65:741–747. [PubMed: 18541794]
15. Fregni F, Boggio PS, Mansur CG, et al. Transcranial direct current stimulation of the unaffected hemisphere in stroke patients. *Neuroreport.* 2005; 16:1551–1555. [PubMed: 16148743]
16. Boggio PS, Nunes A, Rigonatti SP, Nitsche MA, Pascual-Leone A, Fregni F. Repeated sessions of noninvasive brain DC stimulation is associated with motor function improvement in stroke patients. *Restor Neurol Neurosci.* 2007; 25:123–129. [PubMed: 17726271]
17. Ago T, Kitazono T, Ooboshi H, et al. Deterioration of pre-existing hemiparesis brought about by subsequent ipsilateral lacunar infarction. *J Neurol Neurosurg Psychiatry.* 2003; 74:1152–1153. [PubMed: 12876260]
18. Calautti C, Baron JC. Functional neuroimaging studies of motor recovery after stroke in adults: a review. *Stroke.* 2003; 34:1553–1566. [PubMed: 12738893]
19. Foltys H, Krings T, Meister IG, et al. Motor representation in patients rapidly recovering after stroke: a functional magnetic resonance imaging and transcranial magnetic stimulation study. *Clin Neurophysiol.* 2003; 114:2404–2415. [PubMed: 14652101]
20. Cramer SC, Crafton KR. Somatotopy and movement representation sites following cortical stroke. *Exp Brain Res.* 2006; 168:25–32. [PubMed: 16096783]
21. Perez MA, Cohen LG. The corticospinal system and transcranial magnetic stimulation in stroke. *Top Stroke Rehabil.* 2009; 16:254–269. [PubMed: 19740731]
22. Lotze M, Beutling W, Loibl M, et al. Contralesional motor cortex activation depends on ipsilesional corticospinal tract integrity in well-recovered subcortical stroke patients. *Neurorehabil Neural Repair.* 2012; 26:594–603. [PubMed: 22140195]

23. Munoz Maniega S, Cvorov V, Chappell FM, et al. Changes in NAA and lactate following ischemic stroke: a serial MR spectroscopic imaging study. *Neurology*. 2008; 71:1993–1999. [PubMed: 19064881]
24. Kang DW, Roh JK, Lee YS, Song IC, Yoon BW, Chang KH. Neuronal metabolic changes in the cortical region after subcortical infarction: a proton MR spectroscopy study. *J Neurol Neurosurg Psychiatry*. 2000; 69:222–227. [PubMed: 10896697]
25. Kobayashi M, Takayama H, Suga S, Mihara B. Longitudinal changes of metabolites in frontal lobes after hemorrhagic stroke of basal ganglia: a proton magnetic resonance spectroscopy study. *Stroke*. 2001; 32:2237–2245. [PubMed: 11588307]
26. Cirstea MC, Brooks WM, Craciunas SC, et al. Primary motor cortex - a functional MRI-guided proton magnetic resonance spectroscopic study. *Stroke*. 2011; 42:1004–1009. [PubMed: 21330627]
27. Moffett JR, Ross B, Arun P, Madhavarao CN, Namboodiri AM. N-Acetylaspartate in the CNS: from neurodiagnostics to neurobiology. *Prog Neurobiol*. 2007; 81:89–131. [PubMed: 17275978]
28. Hao X, Xu D, Bansal R, et al. Multimodal magnetic resonance imaging: The coordinated use of multiple, mutually informative probes to understand brain structure and function. *Human brain mapping*. 2013; 34:253–271. [PubMed: 22076792]
29. Brunnstrom S. Motor testing procedures in hemiplegia: based on sequential recovery stages. *Physical therapy*. 1966; 46:357–375. [PubMed: 5907254]
30. Craciunas CS, Brooks MW, Nudo RJ, et al. Motor and premotor cortices in subcortical stroke: proton magnetic resonance spectroscopy measures and arm motor impairment. *Neurorehabil Neural Repair*. 2013; XX(X):1–10.
31. Schouten EA, Schiemanck SK, Brand N, Post MW. Long-term deficits in episodic memory after ischemic stroke: evaluation and prediction of verbal and visual memory performance based on lesion characteristics. *J Stroke Cerebrovasc Dis*. 2009; 18:128–138. [PubMed: 19251189]
32. Fazekas F, Chawluk JB, Alavi A, Hurtig HI, Zimmerman RA. MR signal abnormalities at 1.5 T in Alzheimer's dementia and normal aging. *AJR American journal of roentgenology*. 1987; 149:351–356. [PubMed: 3496763]
33. Smith SM, Zhang Y, Jenkinson M, et al. Accurate, robust, and automated longitudinal and cross-sectional brain change analysis. *Neuroimage*. 2002; 17:479–489. [PubMed: 12482100]
34. Heller A, Wade DT, Wood VA, Sunderland A, Hewer RL, Ward E. Arm function after stroke: measurement and recovery over the first three months. *J Neurol Neurosurg Psychiatry*. 1987; 50:714–719. [PubMed: 3612152]
35. Geyer S, Matelli M, Luppino G, Zilles K. Functional neuroanatomy of the primate isocortical motor system. *Anat Embryol (Berl)*. 2000; 202:443–474. [PubMed: 11131014]
36. Duvernoy, H., et al. *The Human Brain: Surface, Three-Dimensional Section Anatomy and MRI*. Springer-Verlag; New York, NY: 1991.
37. Provencher SW. Automatic quantitation of localized in vivo ¹H spectra with LCMoDel. *NMR Biomed*. 2001; 14:260–264. [PubMed: 11410943]
38. Lotze M, Markert J, Sauseng P, Hoppe J, Plewnia C, Gerloff C. The role of multiple contralesional motor areas for complex hand movements after internal capsular lesion. *J Neurosci*. 2006; 26:6096–6102. [PubMed: 16738254]
39. Newton JM, Ward NS, Parker GJ, et al. Non-invasive mapping of corticofugal fibres from multiple motor areas--relevance to stroke recovery. *Brain : a journal of neurology*. 2006; 129:1844–1858. [PubMed: 16702192]
40. Ghosh S, Porter R. Morphology of pyramidal neurones in monkey motor cortex and the synaptic actions of their intracortical axon collaterals. *The Journal of physiology*. 1988; 400:593–615. [PubMed: 3418537]
41. Ward NS. The neural substrates of motor recovery after focal damage to the central nervous system. *Arch Phys Med Rehabil*. 2006; 87:S30–35. [PubMed: 17140877]
42. Dancause N, Barbay S, Frost SB, et al. Extensive cortical rewiring after brain injury. *J Neurosci*. 2005; 25:10167–10179. [PubMed: 16267224]

43. Leocani L, Cohen LG, Wassermann EM, Ikoma K, Hallett M. Human corticospinal excitability evaluated with transcranial magnetic stimulation during different reaction time paradigms. *Brain : a journal of neurology*. 2000; 123(Pt 6):1161–1173. [PubMed: 10825355]
44. Johansen-Berg H, Matthews PM. Attention to movement modulates activity in sensori-motor areas, including primary motor cortex. *Exp Brain Res*. 2002; 142:13–24. [PubMed: 11797080]
45. Bates TE, Strangward M, Keelan J, Davey GP, Munro PM, Clark JB. Inhibition of N-acetylaspartate production: implications for 1H MRS studies in vivo. *Neuroreport*. 1996; 7:1397–1400. [PubMed: 8856684]
46. Willis DE, Twiss JL. The evolving roles of axonally synthesized proteins in regeneration. *Curr Opin Neurobiol*. 2006; 16:111–118. [PubMed: 16418002]
47. Hinman JD, Rasband MN, Carmichael ST. Remodeling of the axon initial segment after focal cortical and white matter stroke. *Stroke*. 2013; 44:182–189. [PubMed: 23233385]
48. Schafer DP, Jha S, Liu F, Akella T, McCullough LD, Rasband MN. Disruption of the axon initial segment cytoskeleton is a new mechanism for neuronal injury. *The Journal of neuroscience : the official journal of the Society for Neuroscience*. 2009; 29:13242–13254. [PubMed: 19846712]
49. Seitz RJ, Azari NP, Knorr U, Binkofski F, Herzog H, Freund HJ. The role of diaschisis in stroke recovery. *Stroke*. 1999; 30:1844–1850. [PubMed: 10471434]
50. Frost SB, Barbay S, Friel KM, Plautz EJ, Nudo RJ. Reorganization of remote cortical regions after ischemic brain injury: a potential substrate for stroke recovery. *Journal of neurophysiology*. 2003; 89:3205–3214. [PubMed: 12783955]
51. Clarkson AN, Clarkson J, Jackson DM, Sammut IA. Mitochondrial involvement in transhemispheric diaschisis following hypoxia-ischemia: Clomethiazole-mediated amelioration. *Neuroscience*. 2007; 144:547–561. [PubMed: 17112678]
52. Dobkin JA, Levine RL, Lagreze HL, Dulli DA, Nickles RJ, Rowe BR. Evidence for transhemispheric diaschisis in unilateral stroke. *Archives of neurology*. 1989; 46:1333–1336. [PubMed: 2590018]
53. Baslow MH. N-acetylaspartate in the vertebrate brain: metabolism and function. *Neurochem Res*. 2003; 28:941–953. [PubMed: 12718449]
54. Liang Z, Zeng J, Liu S, et al. A prospective study of secondary degeneration following subcortical infarction using diffusion tensor imaging. *Journal of neurology, neurosurgery, and psychiatry*. 2007; 78:581–586.
55. Kraemer M, Schormann T, Hagemann G, Qi B, Witte OW, Seitz RJ. Delayed shrinkage of the brain after ischemic stroke: preliminary observations with voxel-guided morphometry. *J Neuroimaging*. 2004; 14:265–272. [PubMed: 15228769]
56. Navarro X, Vivo M, Valero-Cabre A. Neural plasticity after peripheral nerve injury and regeneration. *Prog Neurobiol*. 2007; 82:163–201. [PubMed: 17643733]
57. Schallert T, Leasure JL, Kolb B. Experience-associated structural events, subependymal cellular proliferative activity, and functional recovery after injury to the central nervous system. *J Cereb Blood Flow Metab*. 2000; 20:1513–1528. [PubMed: 11083226]
58. Bradnam LV, Stinear CM, Barber PA, Byblow WD. Contralesional Hemisphere Control of the Proximal Paretic Upper Limb following Stroke. *Cerebral Cortex*. 2011
59. Hattingen E, Lanfermann H, Menon S, et al. Combined 1H and 31P MR spectroscopic imaging: impaired energy metabolism in severe carotid stenosis and changes upon treatment. *Magma*. 2009; 22:43–52. [PubMed: 18855032]
60. Wieloch T, Nikolich K. Mechanisms of neural plasticity following brain injury. *Curr Opin Neurobiol*. 2006; 16:258–264. [PubMed: 16713245]

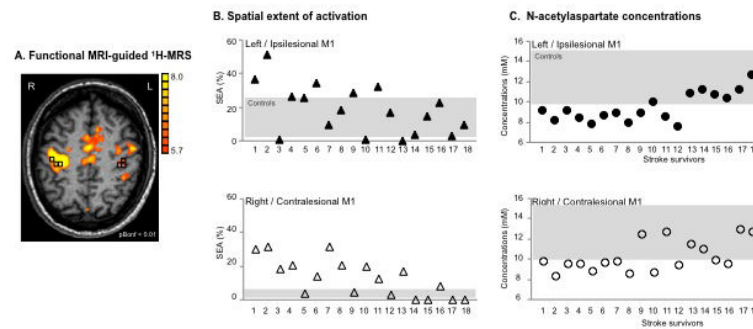


Fig. 1.

(A) Motor-related cortical activation during a handgrip task executed with the impaired right hand in a 45-year old patient who had experienced infarct involving the left basal ganglia and corona radiata (Patient 7, Table 1). Spectroscopic voxels (black squares) were selected in the hand knob area (based on M1 activation and/or anatomical landmarks in case the activation tended to zero). The front of the brain is upwards. L=left, R=right. (B) Spatial extent of M1 activation during handgrip executed with the impaired hand (%) and (C) NAA concentrations (mM) in both ipsilesional (upper row, closed symbols) and contralesional (lower row, open symbols) M1 are shown for individual patient. Stroke survivors are ranked by FMUE scores (see Table 1, with #1, no arm motor impairment; #18, severely impaired). Grey rectangles signify the range of spatial extent activation (B) and NAA concentrations (C) in left (upper row) and right (lower row) M1 in healthy controls.

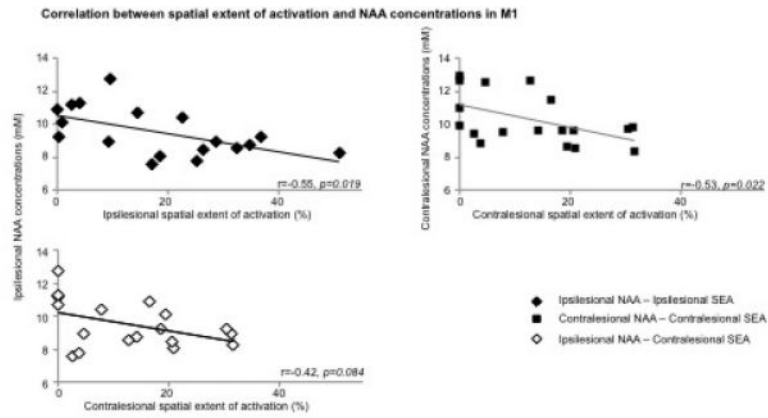


Fig. 2. Scatterplot of Spearman correlations between (A) ipsilesional NAA concentrations (mM) and ipsilesional (top row, black diamond, $r=-0.55$, $p=0.02$) and contralateral (low row, white diamond, $r=-0.42$, $p=0.08$) handgrip-related spatial extent of activation (SEA, %), and between (B) NAA and SEA within contralateral M1 (square, $r=-0.53$, $p=0.02$) in stroke patients.

Table 1

Demographic and clinical stroke characteristics.

Patient	Age/Sex	Time after stroke (mo)	Lesion location	Lesion volume (mm ³)	Fazekas	FMUE
1	61/M	24	L / BG, IC, CR	25,339.9	1	10
2	58/M	27	R / PLIC, BG	553.7	1	24
3	59/M	144	L / PLIC, BG	1,451.9	0	25
4	44/F	106	L / BG, IC, CR	17,881.3	0	26
5	56/F	6	R / PLIC, BG	6,902.9	0	29
6	61/M	12	L/Pons	1,445.8	0	30
7	45/M	27	L / BG, CR	180.4	0	36
8	71/M	26	R / PLIC, BG	1,192.7	1	37
9	73/M	60	R / ALIC, BG	21,960.35	0	41
10	65/M	36	R / BG, CR	271.6	1	42
11	61/F	27	L / CP	2357.2	1	50
12	56/M	23	L / ALIC	490.4	1	50
13	46/F	8	R / BG	737.4	1	58
14	54/F	12	L /ALIC/genu, BG	450.0	0	60
15	48/F	11	L / PLIC, BG	60,450.3	0	61
16	46/M	52	L / PLIC, BG	740.0	0	63
17	68/M	63	L / PLIC, T	1,449.3	0	65
18	57/M	6	L / BG, CR	10501.9	1	66

M, male; F, female; mo, months; L, left; R, right; BG, basal ganglia; CR, corona radiata; PLIC, posterior limb internal capsule; ALIC, anterior limb internal capsule; CP, cerebral peduncle; T, thalamus; mm=millimeters; Fazekas scale for white matter hyperintensities FMUE (0 to 3, 0 and 1 normal for elderly), Fugl-Meyer Upper Extremity, normal=66, as recorded at the recruitment into study, Fazekas scale (normal for elderly people=0 and 1).

Table 2

Spearman correlations (r , p -value) between primary motor cortex (M1) outcomes, measured bilaterally, and clinical variables in stroke survivors.

	<i>Fugl-Meyer Upper Extremity</i>	<i>Lesion volume</i>	<i>Global grey matter volume</i>	<i>Time after stroke</i>
<i>N-acetylaspartate (mM)</i>				
Ipsilesional	0.63, .005	0.42, .08	0.25, .3	-0.13, .6
Contralesional	0.55, .02	-0.02, .9	0.23, .4	-0.09, .7
<i>Spatial extent of activation (%)</i>				
Ipsilesional	-0.48, .04	-0.05, .8	0.04, .9	-0.04, .9
Contralesional	-0.77, <.01	0.11, .6	0.15, .5	0.33, .2

Table 3

Comparisons of mean (SD) of primary motor cortex (M1) outcomes in patients with left vs. right stroke and with PLIC vs. ALIC stroke.

	<i>Left hemisphere stroke (n=12, FMUE=45.2±19.1, time after stroke=32.7±28.4mo)</i>	<i>Right hemisphere stroke (n=6, FMUE=38.5±11.6, time after stroke=46.8±51.6mo)</i>	<i>p-value</i>
<i>N-acetylaspartate (mM)</i>			
Ipsilesional	9.6±1.6	9.3±1.1	.7
Contralesional	11.3±1.6	10.1±1.5	.8
<i>Spatial extent of activation (%)</i>			
Ipsilesional	22.5±14.4		.1
Contralesional	11.7±11.9	15.7±10.3	.5
	<i>PLIC stroke (n=7, FMUE=43.4±18.8, time after stroke=47.0±47.4mo)</i>	<i>ALIC stroke (n=3, FMUE=50.3±9.5, time after stroke=32.0±24.9mo)</i>	<i>p-value</i>
<i>N-acetylaspartate (mM)</i>			
Ipsilesional	9.3±1.4	9.3±1.2	.9
Contralesional	9.6±1.6	10.9±1.5	.2
<i>Spatial extent of activation (%)</i>			
Ipsilesional	19.3±16.8	16.6±12.4	.8
Contralesional	11.8±12.1	2.4±2.2	.2

n, number of patients; FMUE, Fugl-Meyer Upper Extremity, mo, months